

Sensitivity studies applied to a two-dimensional resistivity model from the Central Andes

Katrin Schwalenberg,^{1,*} Volker Rath^{2,†} and Volker Haak¹

¹GeoForschungsZentrum Potsdam, Telegrafenberg, 14473 Potsdam, Germany. E-mail: katrin@physics.utoronto.ca

²Fachrichtung Geophysik, Freie Universität Berlin, Malteser Str. 74-100, 12249 Berlin, Germany

Accepted 2002 March 7. Received 2001 October 1; in original form 2001 March 27

SUMMARY

Long-period magnetotelluric (MT) data have been collected along an E–W profile across the Central Andes in Northern Chile and Southern Bolivia. A 2-D resistivity model explaining these data was found by inverse modelling. The model includes a prominent conductivity anomaly in the backarc of the South American subduction zone below the Bolivian Altiplano. Another, comparatively localized anomaly occurs beneath the Precordillera in the forearc. The enhanced conductivity in the backarc correlates with reflective zones, low seismic velocities and high seismic attenuation. In contrast, no correlation can be found in the forearc. A strong seismic reflector in context with the down-going slab, and another reflector in the middle crust below the Pre- and Western Cordillera do not coincide with anomalous conductivity.

Other 2-D models may also be consistent with the data. We applied different techniques to find the range of relevant models. One simple but useful approach is the direct use of the sensitivity matrix containing the partial derivatives of the data with respect to the model parameters. The sensitivity of the model parameters to the data or data subsets can be visualized by calculating columnwise sums from the sensitivity matrix. These sensitivities may be used to indicate model parameters that are less resolved by the data and thus should not form part of an interpretation. Another approach is to perform systematic studies to establish the validity of geologically important features of the model. These studies comprise forward modelling and the use of *a priori* information. Combining all approaches generates a more complete assessment of the principal model features.

We conclude that a minimum depth extent of the Altiplano conductor can be specified as approximately 50 km. Low sensitivity in the forearc beneath the Longitudinal Valley indicates a limited structure resolution, and therefore may explain the absence of a conductive slab in the model. The existence of the localized conductor below the Precordillera can be established by high sensitivity. Finally, we included the two seismic reflectors in the forearc as *a priori* information in the inversion process. As a result the absence of a conductive slab in the model is probably a result of low sensitivity, but cannot be totally excluded. A conductive zone coinciding with the strong reflector below the Pre- and Western Cordillera is not manifested by the MT data.

Key words: 2-D inversion, Central Andes, magnetotellurics, sensitivity studies, subduction zones.

1 INTRODUCTION

Magnetotelluric (MT) measurements have been carried out in Northern Chile and Southern Bolivia to examine the conductivity

structure of the Central Andes. The main result of these measurements is a huge crustal conductivity anomaly in the backarc of the South American subduction regime below the Bolivian Altiplano. This anomaly is most probably caused by partial melts in context with saline fluids. Data analysis, 2-D inversion results and possible causes of enhanced conductivity have been discussed in Brasse *et al.* (2002). However, the inverse solution is not unique. Here we present an extensive sensitivity analysis to characterize the uncertainties in the calculated models, and to better quantify the correlation with available seismic data.

*Now at: Department of Physics, University of Toronto, 60, St George St, Toronto M5S1A7, Canada.

†Now at: Angewandte Geophysik, Rheinisch-Westfälische Technische Hochschule Aachen. Lochnerstr. 4-20, 52056 Aachen, Germany.

In magnetotellurics a model can be constructed either by forward modelling or by inversion. Forward modelling is a unique procedure of calculating synthetic data for a given electrical conductivity or resistivity distribution. Inverse modelling usually describes an iterative process of calculating a resistivity model from given measured data—a procedure that usually delivers a range of possible models because of the inherent ill-posedness (Hadamard 1923) of the non-linear inverse problem. A mathematically unique solution may exist, but false physical assumptions (e.g. dimensionality), statistical and systematic errors in the data, or inadequate parametrization of the model may prevent it from being found. Inversion is stabilized by applying appropriate constraints on the solution, e.g. by requiring the solution to minimize certain functionals in addition to the standard least-squares data fit. This approach is known as regularization (Tikhonov & Arsenin 1979). It differs from the often presented, and elaborate statistical background of Bayesian inversion (Tarantola & Valette 1982a,b) by the determination of a free trade-off parameter instead of requiring the solution to meet any given *a priori* information. Stable models can be calculated by this method, but even in this case the resulting models may or may not represent the true resistivity distribution at depth. Furthermore, induction theory tells us that the relation between data and model parameters is non-linear. This implies that the model parameters cannot all be equally well determined, even from error-free data. To gain a physically and geologically reasonable model, it is therefore necessary not only to solve an ill-posed mathematical problem, but also to study carefully the sensitivity of the data, or subsets of them, with respect to changes in the important model parameters. After formally studying the relation between the data and the model itself using sensitivity and derived concepts, it is useful and obvious to compare the distribution of subsurface resistivity with other geophysical models—provided they are available. This motivates the discussion as to whether agreement exists—or should exist—between the different physical properties.

We will present inversion results and a 2-D sensitivity analysis of data from the Central Andes. Fig. 1 shows a topographic map with all sites in the measurement area. For the 2-D modelling data from 32 sites along the ANCORP profile at 21°S (ANdean Continental Research Programme, a large active and passive seismic experiment (ANCORP Working Group 1999)) have been selected. This profile

covers the main morphological units of the Central Andes. To interpret the data we used the 2-D inversion code of Mackie *et al.* (1997) (see also Rodi & Mackie 2001). With this code the least-squares solution is regularized by a roughness penalty realized by a difference operator, acting in the vertical and the horizontal direction. The relative weight given to the data fit and the model smoothness is controlled by a trade-off parameter that influences the inversion result significantly, and has to be chosen carefully. Nevertheless, the obtained solution is only one possibility from a multidimensional model space, so the inversion problem remains ambiguous.

We will address the problem of non-uniqueness from a linear and a non-linear point of view. The linear approach is based on the sensitivity matrix. The matrix is obtained automatically when linearizing the forward problem within the inversion process, but in fact it can be calculated for any given model. The elements of the matrix are the partial derivatives of the data with respect to the model parameters. It is a measure of how small model distortions influence the data. As a picture it can be used to show the information content of the data set. In a typical 2-D MT problem this picture is complicated because of the sheer size of the sensitivity matrix. We therefore calculated columnwise sums of the sensitivity matrix or its subspaces, and added a suitable weighting for the respective grid elements. This enables us to visualize the average sensitivities on the model grid.

The non-linear approach comprises systematic forward modelling studies—a trial and error process favoured by many interpreters, because it may identify models inaccessible to linear inversion. The parameters of distinct model parts were varied in a systematic manner until the fit between the model prediction and observations becomes worse. However, because the 2-D MT problem is non-linear and the parameters that define the model are by no means independent, a forward study is of only limited significance.

A priori information that might be motivated by geology and other geophysical investigations can be utilized in both the linear and the non-linear approach. They are useful for the construction of the forward model, or they can be incorporated in the inversion process. Starting the iterative process with this option, Mackie's algorithm then seeks a solution close to the *a priori* model. As a result, structural information from the *a priori* model are maintained in the inversion result. If compatible with the data, this will lead

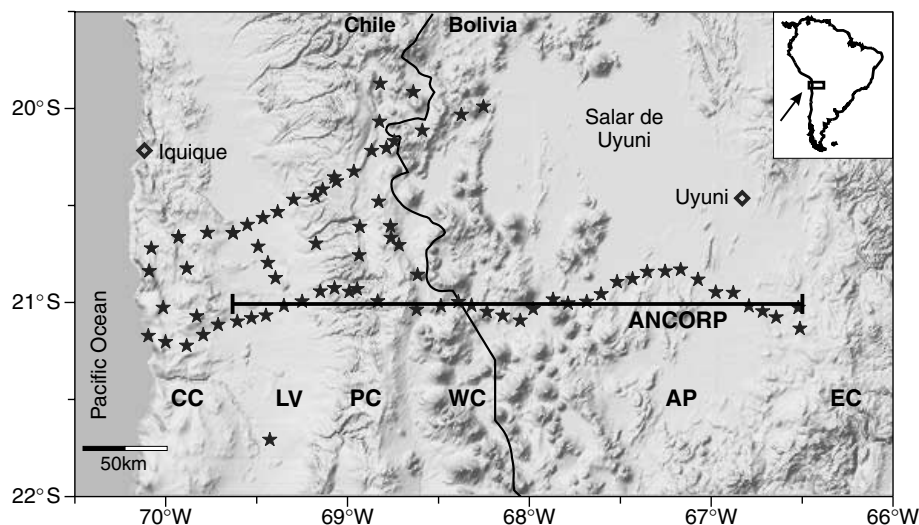


Figure 1. Topographic map of the Central Andes. Stars indicate MT sites. The thick line marks the position of the ANCORP profile at 21°S. CC: Coastal Cordillera, LV: Longitudinal Valley, PC: Precordillera, WC: Western Cordillera, AP: Altiplano, EC: Eastern Cordillera.

to minor changes in the results. If this is not the case, convergence may be inhibited, or incompatible structures may be compensated by artefacts, keeping the conductance equal in the region of interest. We applied this option in using two seismic bright-spots in the forearc as *a priori* information, and checking their conformity with the MT data.

Linear analysis based on the sensitivity matrix is by definition only of value close to the derived model. Statements concerning alternative solutions far away from the linear model under consideration can only be made using a non-linear search. In this paper we will show that a combination of the two approaches is adequate for dealing with the problem of non-uniqueness of the inverse solution.

2 2-D INVERSION

The 2-D inversion code of Mackie *et al.* (1997) was used to model the data along the ANCORP profile at 21°S (see Fig. 1). As input data we used TE and TM mode data in a period range between 18 and 17 500 s. We applied a minimum error floor of 20 per cent in $\log \rho_a$ and 1° in φ to down-weight the apparent resistivities with respect to the phases.

The 2-D interpretation of the data has been justified by a dimensionality analysis, showing that the data can be treated as 2-D in a first step for most sites on the profile (Brasse *et al.* 2002). The data from the Altiplano support a simpler, i.e. approximately 1-D resistivity distribution. The westernmost sites on the ANCORP profile are not 2-D and were not included in the model.

In Mackie's code the objective function, which has to be minimized in each iteration, is given by

$$\Phi = \Phi_d + \tau \cdot \Phi_m. \quad (1)$$

This is a linear combination of the χ^2 -function:

$$\Phi_d = \left\| \frac{\mathbf{d} - \mathbf{f}(\mathbf{m})}{\sigma} \right\|^2 \quad (2)$$

with \mathbf{d} = data vector, $\mathbf{f}(\mathbf{m})$ = forward solution of model \mathbf{m} , σ = data errors, and a Tikhonov regularization term that is realized by either a first- or second-order operator \mathbf{D} calculating differences between adjacent grid elements in vertical and horizontal directions:

$$\Phi_m = \|\mathbf{D}(\mathbf{m} - \mathbf{m}_{\text{apr}/0})\|^2. \quad (3)$$

The regularization term has a smoothing effect on the inversion result; more precisely, the roughness operator \mathbf{D} acts on the difference between the actual model \mathbf{m} and an optionally given *a priori* model \mathbf{m}_{apr} which in the version of the code used can differ from the starting model \mathbf{m}_0 . The final model does depend on the structural information of the *a priori* model, which may lead to biased inversion results if the *a priori* information is inconsistent with the data. For this reason we used as a starting model a 25 Ω m half-space with the ocean (0.3 Ω m)—the dominant *a priori* information—incorporated. Exceptions are described in Sections 4 and 5 where we modify the starting model to check the consistency of *a priori* information with the MT data.

The inversion results depend significantly on the value of a trade-off parameter τ , which controls the balance between data fit and model roughness. In Mackie's code the trade-off parameter is fixed for each inversion run. To find an appropriate choice for τ we started the inversion several times, increasing τ stepwise by orders of magnitude. Fig. 2 shows three inversion results with $\tau = 1, 10$ and 100, respectively, and where the first difference operator was applied. Only the first 100 km of the central part of the model, which is

covered by measuring sites, is shown. The inversion was stopped after 30 iterations, when the algorithm had already converged to a constant level. For higher τ , greater emphasis is put on the regularization term, and hence the resulting model is smoother, while the normalized rms error

$$\text{rms} = \sqrt{\frac{1}{N} \Phi_d} \quad (4)$$

can be reduced by allowing more structure in the model. However, when τ is too small, the algorithm shows oscillatory behaviour and even may become unstable, which means that no reliable model can be found. This kind of systematic test was also carried out for the second-order difference operator (results not shown here). To determine an appropriate choice for τ we plotted in Fig. 3 the χ^2 -function (Φ_d) against the model roughness (Φ_m) on a double logarithmic scale for the 15th iteration of different inversion runs with varying τ . The curve obtained shows a typical L-form (Hansen 1998), which is also observable for the remaining iterations. An exception is when τ was chosen too small. The algorithm may become unstable causing the data misfit to oscillate or even diverge in the course of the preceding inversion. Following the idea of a minimum structure model (de Groot-Hedlin & Constable 1990) we are seeking a model that represents a compromise between the data fit and the model smoothness. We think that for the given data and model parametrization this is realized for $\tau = 10$, because the data fit degrades significantly with increasing τ while smaller τ results in rougher models. Furthermore, in Mackie's code a Marquardt-like regularization factor has to be set in the objective function that stabilizes the inversion process in early iterations. This factor we fixed at a small value of 0.001 for all inversion results presented here.

In the following we treat the reference model in Fig. 2 (middle) as our preferred inversion result, and name it the ANCORP model. The outstanding feature of the inversion is a huge conductivity anomaly below the Bolivian Altiplano (Altiplano conductor). With this model a good fit to the data can be obtained, as described in more detail elsewhere (see Brasse *et al.* 2002). The relatively high rms of 3.3 can be explained by the effect of small, near-surface inhomogeneities that shift the apparent resistivity curves, while leaving the phases undisturbed. This effect is commonly known as static shift, and can be observed at several sites. The original code has been modified to allow the correction of static shifts. When enabling this option at late iterations an rms of 1.7 can be obtained, while the resulting model itself remains comparable with the ANCORP reference model.

A number of general questions from this inversion result arise. How trustworthy are the obtained model structures? Is it possible to specify the vertical extension of the Altiplano conductor? Do the MT results coincide with other, namely seismic results? We address these questions through a variety of sensitivity studies described below.

3 LINEAR SENSITIVITY STUDIES

In the previous section we found a minimum structure inversion model. This model is one of a very large number of geologically reasonable models that explain the observed data to within a given data misfit. Sensitivity studies are therefore required to make further statements concerning the model resolution.

We will start with the introduction of a simple but nevertheless useful approach that makes direct use of the Jacobian matrix. This matrix is a by-product of linearizing the non-linear forward problem

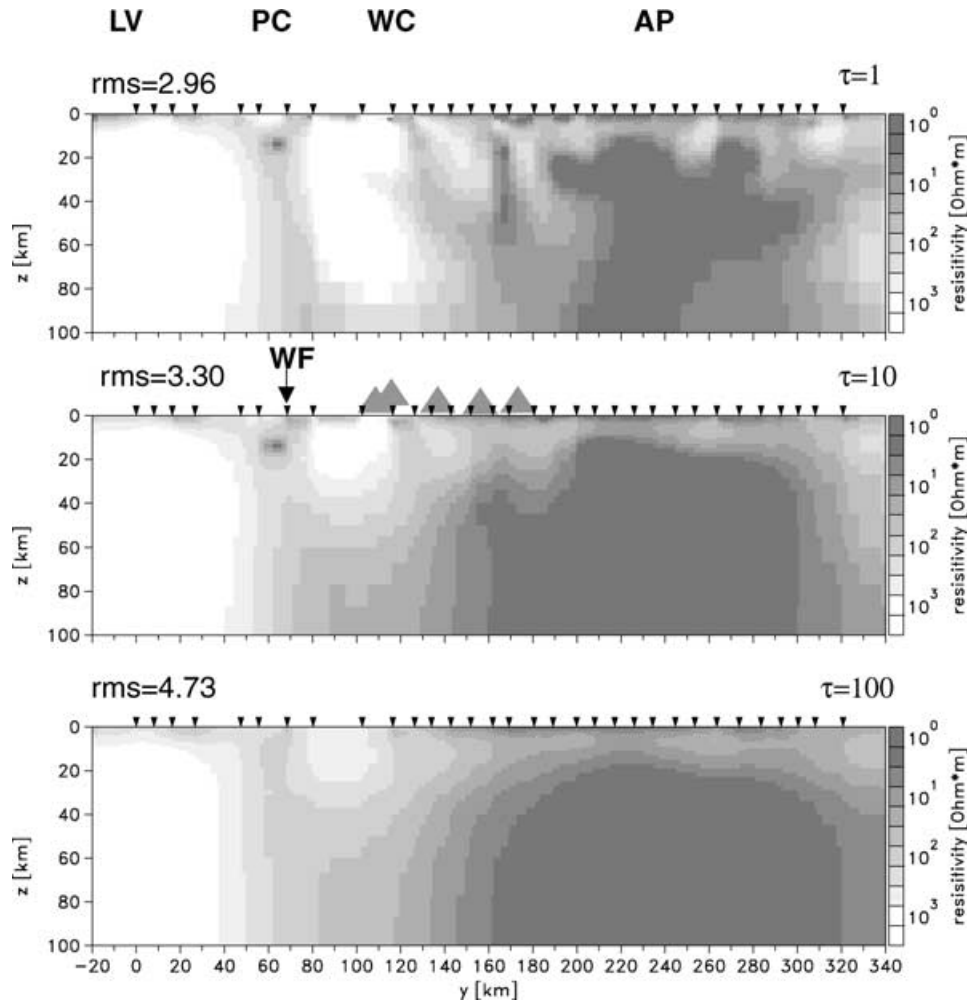


Figure 2. Inversion results with different trade-off parameter τ . With increasing τ the models becomes smoother while the data fit (rms error) worsens. Also marked is the surface position of the West Fissure (WF) and the volcanic arc in the middle figure. For other abbreviations see Fig. 1. The central model is an optimal minimum structure model, and will be used as reference model in this paper (ANCORP model).

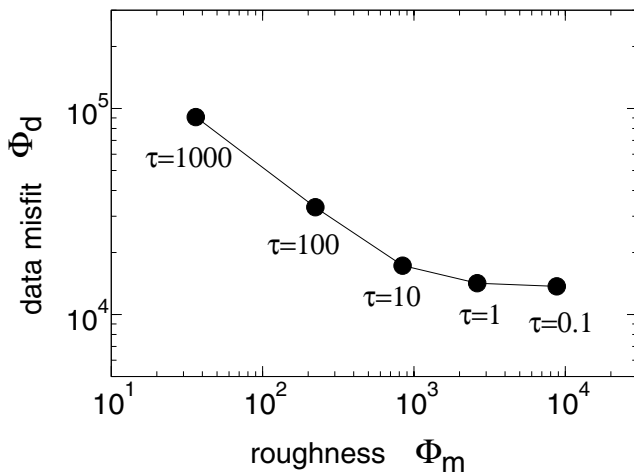


Figure 3. To determine an optimal trade-off parameter the χ^2 misfit function Φ_d has been plotted against model roughness Φ_m in a double logarithmic scale for the 15th iteration resulting in a typical L-form. As an optimal trade-off parameter we choose $\tau = 10$.

into a Taylor series, a common procedure when dealing with non-linear problems. Neglecting higher terms one obtains

$$\mathbf{f}(\mathbf{m}) = \mathbf{f}(\mathbf{m}_0) + \frac{\partial \mathbf{f}}{\partial \mathbf{m}} \delta \mathbf{m} \quad (5)$$

with $\delta \mathbf{m}$ being a small parameter variation. We call $\mathbf{S} = \partial \mathbf{f} / \partial \mathbf{m}$ the sensitivity matrix. Its elements are the partial derivatives of the data with respect to the model parameters. The term sensitive is understood here in a positive sense that infinitesimal parameter variations have an influence on the data. The full space matrix can be written as

$$\mathbf{S} = \begin{bmatrix} \frac{\partial f_1}{\partial m_1} & \frac{\partial f_1}{\partial m_2} & \dots & \frac{\partial f_1}{\partial m_M} \\ \frac{\partial f_2}{\partial m_1} & \frac{\partial f_2}{\partial m_2} & \dots & \frac{\partial f_2}{\partial m_M} \\ \vdots & \vdots & \ddots & \vdots \\ \frac{\partial f_N}{\partial m_1} & \frac{\partial f_N}{\partial m_2} & \dots & \frac{\partial f_N}{\partial m_M} \end{bmatrix}, \quad (6)$$

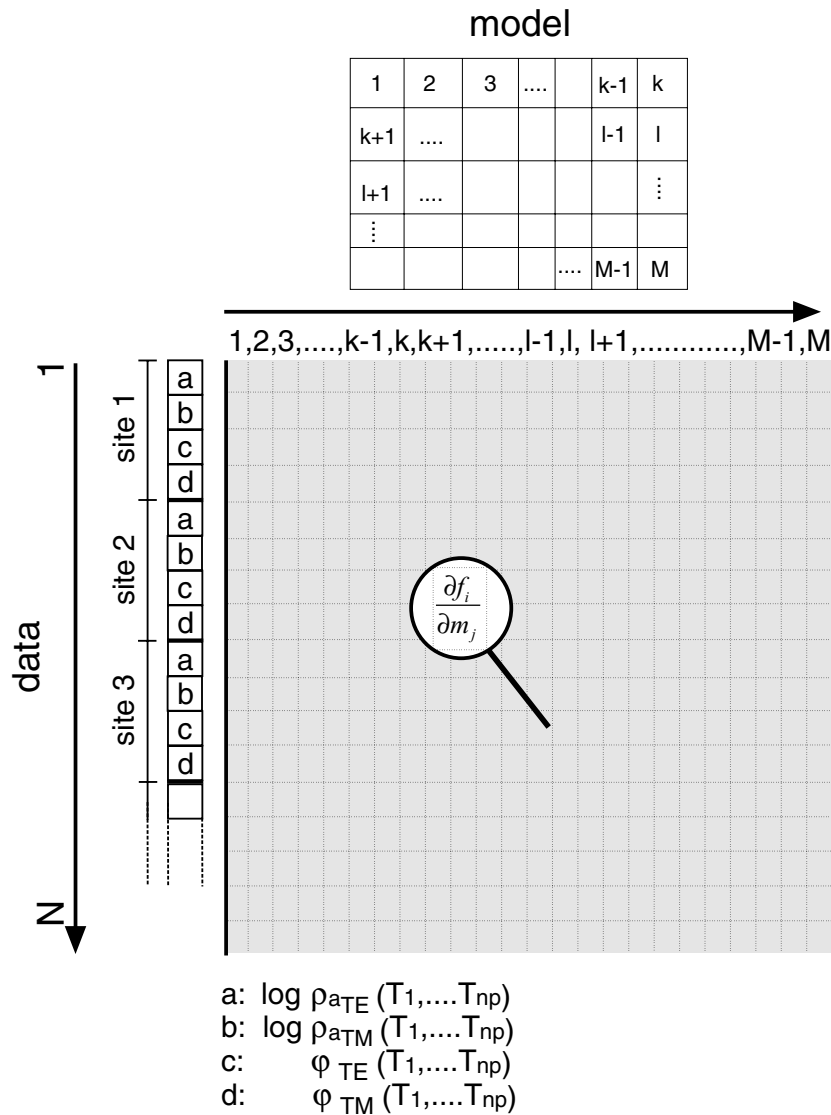


Figure 4. Schematic presentation of the sensitivity matrix. The columns refer to the data space, and have N elements ($N = \text{no of sites} \times \text{no of periods (np)} \times \text{four data types} (\log \rho_{aTE}, \log \rho_{aTM}, \varphi_{TE}, \varphi_{TM})$). The rows contain the whole model parameter vector, namely $\log \rho_j, j = 1, \dots, M$.

where $f_i (i = 1, \dots, N)$ comprises the whole data space, means $(\log \rho_{aTE}, \log \rho_{aTM}, \varphi_{TE}, \varphi_{TM})$ for each site location and period T (TE for tangential electric, TM for tangential magnetic). $m_j (j = 1, \dots, M)$ refers to the logarithm of resistivity of each model element ($\log \rho(y, z)$). Fig. 4 displays a schematic presentation of the sensitivity matrix. Each column contains the derivatives of all data with respect to one specific model parameter. In our example the data are written out site by site. Each site comprises data from the above-mentioned four types of all periods T_1, \dots, T_{np} . The rows of the sensitivity matrix contain the derivatives of one specific datum with respect to all model parameters.

Before we present sensitivities for the ANCORP model we illustrate in Fig. 5 normalized sensitivities for one site on a homogeneous half-space ($30 \Omega \text{ m}$). The simplicity of the data and the model allows us to show the sensitivities separately for resistivities and phases, as well as for TE and TM modes for periods 0.1, 1 and 10 s. It becomes clear how the sensitivity expands spherically with increasing period. In the on-line colour version of Fig. 5, changes in sign indicate whether a positive parameter variation causes an in-

crease or decrease in the resistivities or phases, respectively. These changes are more distinct in the TM mode, which can be explained by the characteristic overshoots at model discontinuities. Absolute sensitivities are shown in the black and white paper version. Also, from the different behaviour of the two modes it may be expected that data from different modes will resolve different features in the model (e.g. Brasse *et al.* 2002).

In a typical 2-D case the calculation of the sensitivity matrix is the most time consuming part of the inversion process. If the sensitivities were calculated by brute force, the forward problem would have to be solved M times. In Mackie's inversion code a cleverer method is applied where the electromagnetic reciprocity theorem is used to decrease the number of forward solutions required (see Madden 1972; Farquharson & Oldenburg 1996; McGillivray & Oldenburg 1990). The storage of the whole, often very large sensitivity matrix can even be avoided completely when modern methods such as conjugate gradients are used to solve the non-linear optimization problem. The sensitivity matrix is then only considered within matrix-vector products (Mackie & Madden 1993; Rodi & Mackie 2001).

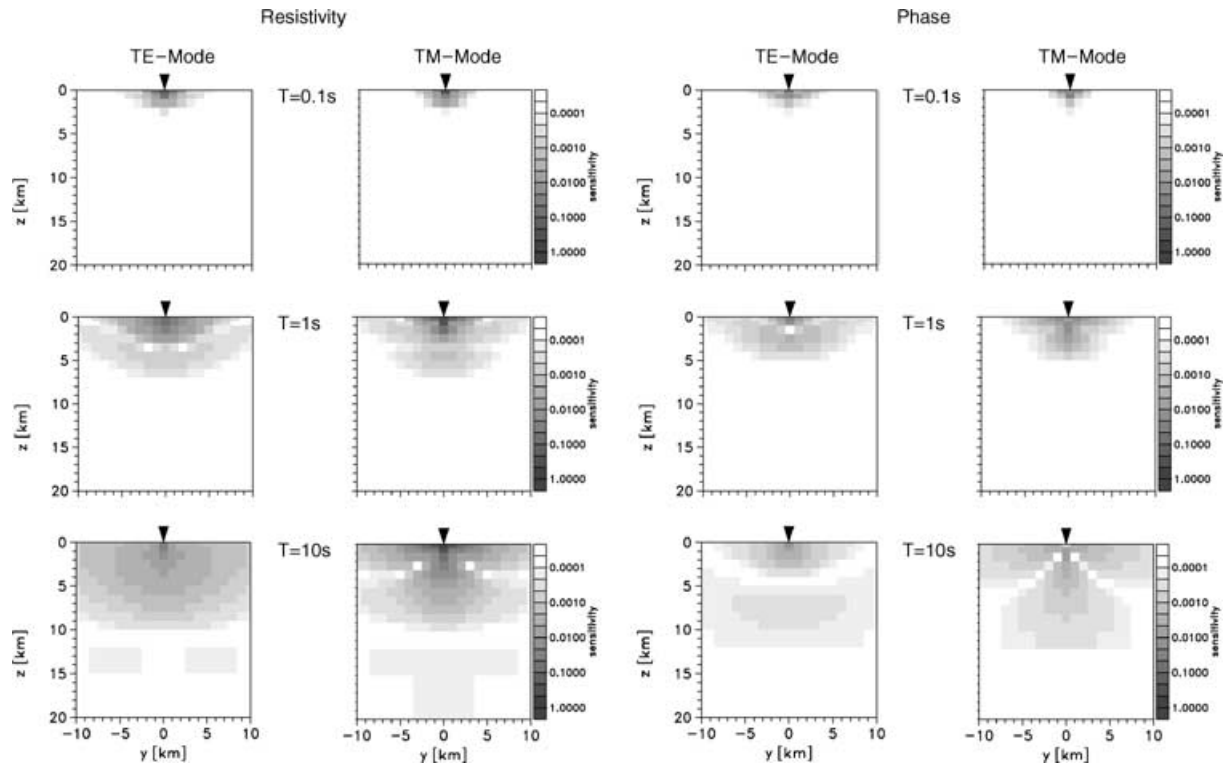


Figure 5. Sensitivities normalized by standard deviation have been calculated for data from one site on a homogeneous half-space. TE and TM mode apparent resistivities and phases for different periods display the increasing induction space with period. A pseudo-logarithmic scale was applied to meet both variance and changes in sign of the sensitivities in the on-line colour version. The black and white paper version shows absolute values.

This is realized in newer versions of Mackie's code, but since this matrix contains valuable information, we used an older version based on the Gauss–Newton method (Björk 1996).

The presentation of 2-D sensitivities raises several difficulties: the dimension of the sensitivity matrix complicates the visualization of the whole matrix. For the model considered here, this matrix has 1492 rows (data) and 6644 columns (parameters). The suggestion we make is to calculate columnwise sums from the sensitivity matrix and assign them to the particular model parameters or grid elements, respectively. The data vector thereby consists of two different types, namely $\log \rho_a$ and φ which vary on different scales. To normalize the sensitivities derived from these two data types we simply divided them by the respective standard deviation σ_i , which also makes them numerically comparable and dimensionless. Furthermore, the sensitivities can be positive and negative and range over several orders of magnitude. We took the absolute values of the sensitivities, because we are mainly interested in whether a model parameter is sensitive to the data or not. We must also allow for the use of a graded grid, as is common in electromagnetic studies. To avoid large grid elements biasing the presentation, we divided the resulting sums by the size of the respective grid element Δ_j . Altogether the resulting sums can be denoted by

$$s_j = \frac{1}{\Delta_j} \sum_i^N \left\| \frac{1}{\sigma_i} \frac{\partial f_i(\mathbf{m})}{\partial m_j} \right\|. \quad (7)$$

Fig. 6(A) shows the sensitivities calculated from the ANCORP model in Fig. 2 (middle). The respective values calculated from eq. (7) were normalized by maximum sensitivity, so the colour codes refer to the fraction of maximum sensitivity. A general decrease of sensitivity with depth can be observed. Some structural informa-

tion is also visible. Below the Longitudinal Valley (LV), and inside the good conductor beneath the Altiplano (AP) the sensitivity decreases more rapidly with depth than elsewhere. Outside the presented model part the sensitivities are low, and only the ocean layer remains sensitive. It should be mentioned that the quantities presented in this figure are calculated from the whole data space. This is a possibility to present average sensitivities. Also shown in Fig. 6 are two applications for these sensitivities (B, C). We follow the ideas of Oldenburg & Li (1999) who derive a depth-of-investigation (DOI) index from alternative resistivity models, which they calculated from IP and DC data. Following their strategy we extract isolines from the sensitivity plot and print them over the resistivity model (Fig. 6B). The model parameter closest to the site locations are the most sensitive ones. For these parameters, small variations cause a static shift effect, which arises along with higher sensitivity. Furthermore, sensitivity generally decreases rapidly with depth, displaying the integrated induction space of the whole data base. We recommend choosing a minimum sensitivity to rule out deeper structures from the interpretation, and therefore obtain a more reliable presentation of the model. However, the choice of this sensitivity limit is an open question requiring further investigation. In this paper we are led to our choice by comparison with forward modelling studies described in the next section, and use the 10^{-4} -isoline to fade out the deeper structures (C).

Instead of summing up the whole data space as described above, subspaces of data can also be considered in eq. (7). The interesting subspaces are easily extracted from the sensitivity matrix. In Fig. 7 only data with periods 18 s (A) or 3300 s (B) were considered. The greater sensitivity of longer periods to deeper structures is clearly visible. Again, the deeper parts below the Longitudinal Valley and the Altiplano remain less well resolved by the data than below the

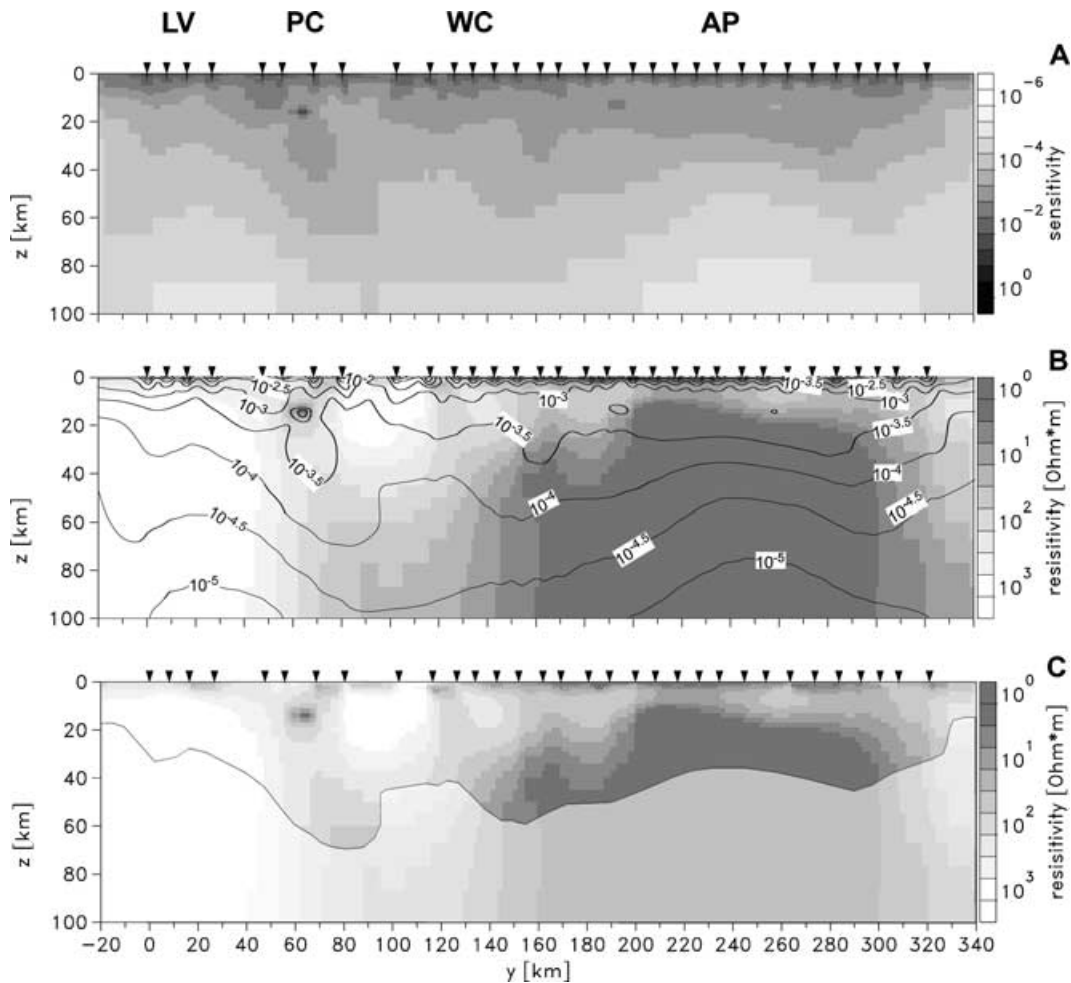


Figure 6. (A) Averaged sensitivities have been calculated from the sensitivity matrix by adding up absolute values of the whole data space. The resulting sums were normalized by standard deviation, grid size, and by maximum sensitivity so that the maximum value is 1. Consequently, the colour code refers to fraction of maximum sensitivity. (B) Isolines have been extracted from A and plotted on to the ANCORP model. A general decrease of sensitivity with depth is visible. Sensitivity decreases faster below the Longitudinal Valley (LV) and Altiplano (AP). The highest sensitivities can be found directly beneath the site locations. In C the 10^{-4} -isoline was used to fade out deeper model structures from interpretation.

Pre- and Western Cordillera. Sensitivities calculated for single sites (TIQ, PAM) mainly present the induction space for the respective site (Figs 7C and D), and also demonstrate sufficient overlap between adjacent sites.

Subspace sensitivities for ρ_a and phase in Figs 8(A) and (B) show that the sensitivities of the two data types are comparable when they are normalized to unit variance. When summing up TE and TM mode data separately (Figs 8C and D) it becomes clear that the TE mode data are less sensitive to structure beneath the Longitudinal Valley. This can be explained by the coastal effect. These sites are near to the Pacific Ocean, which itself is a good conductor, and prevents the currents running parallel to the coast from penetrating to a greater depth. As structural information, the localized conductor below the Precordillera can be associated with high sensitivity in the single-site and single-period presentations, and is very clear in the TE mode data subspace image.

However, the sensitivities are only valid in a linear space close to the model. Therefore, their information content is limited and does not provide ideas concerning alternative models that differ significantly from the respective model. Nevertheless, we believe it is helpful in the discussion of the reliability of inversion results.

4 NON-LINEAR SENSITIVITY STUDIES

In the following we will present systematic studies based on forward modelling and the use of *a priori* information. We call them non-linear sensitivity studies because these tests consider models that differ significantly from our optimal inversion result—the ANCORP model. They were performed in order to check the importance of distinct model features with respect to the data or data subsets. Fig. 9 shows a sensitivity study in the style of Nolasco *et al.* (1998). For three regions, we varied the resistivity values over several orders of magnitude. By solving the forward problem in each case we calculated the rms misfit as a function of resistivity (bottom diagrams). If the resistivity values around the conductor beneath the Precordillera (area A) are varied while the rest of the model is kept unchanged a minimum rms is found for $\rho = 10 \Omega\text{m}$. The value is a factor of 10 higher than the minimum resistivity values in the ANCORP model for the Precordilleran conductor (*cf.* Fig. 6B). In this test a rather large volume was considered so that $10 \Omega\text{m}$ is an average value for area A. When varying the resistivities in area B (top of the Altiplano conductor) the data fit worsens when ρ is smaller than $3 \Omega\text{m}$, while the rms is nearly constant for higher values. The data are insensitive to higher resistivities in this area. A surface-parallel

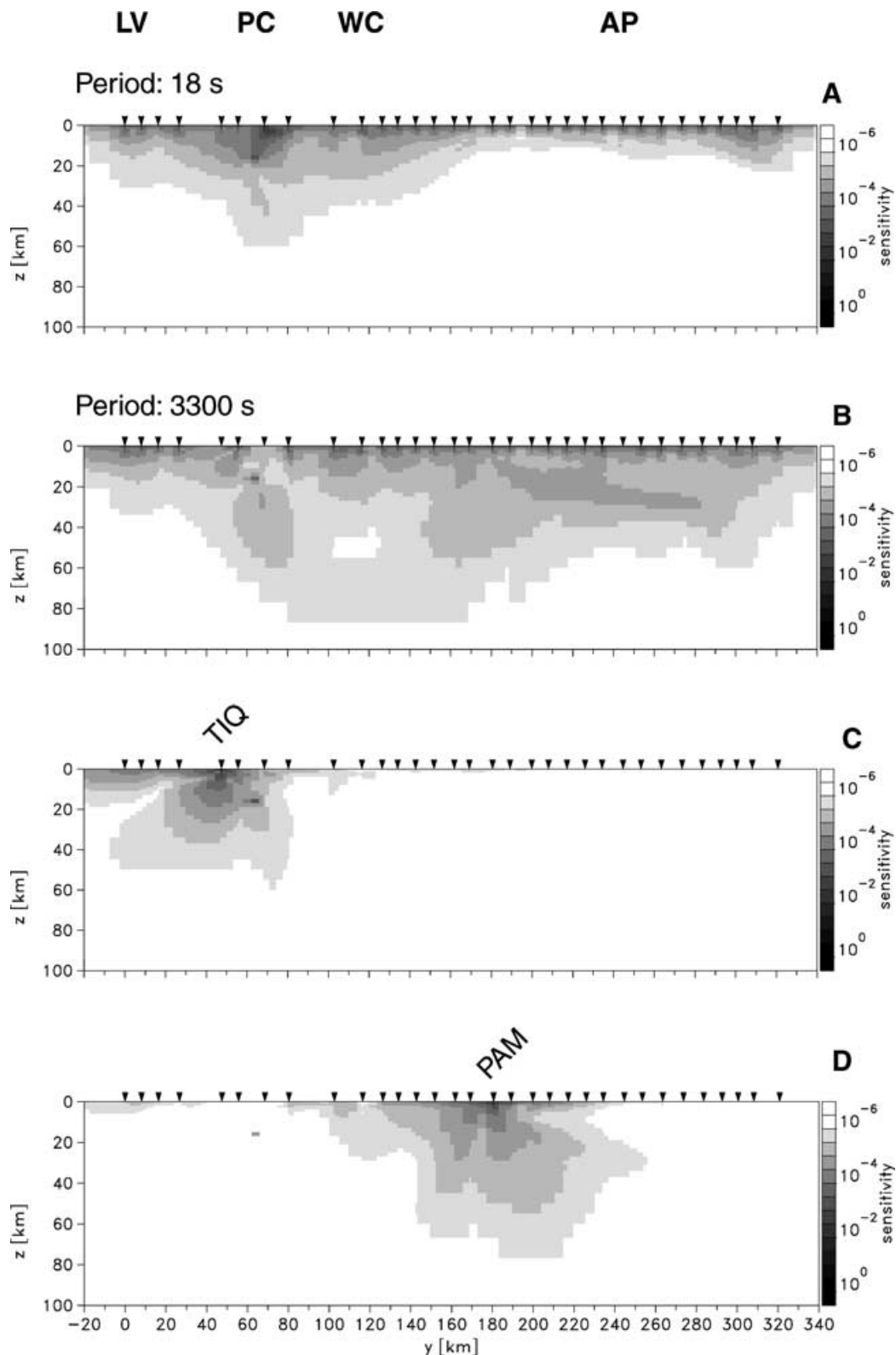


Figure 7. Sensitivities presented here were calculated from data subspaces of the sensitivity matrix. Sensitivities for periods 18 s (A) and 3300 s (B) show that deeper model parts are sensitive to longer periods. Sensitivities plotted for single sites suggest a sufficient overlap between sites (C, D).

upper boundary of the Altiplano anomaly can be excluded. The depth extent of the Altiplano conductor is of particular interest. From our results for region C it is clear that resistivity values above $3 \Omega \text{ m}$ are unlikely. In contrast, the rms error changes little for values

less than $1 \Omega \text{ m}$. If we assume that the resistivities are uniform in the area marked C (which is certainly not the case) the optimum average resistivity value is of order $1 \Omega \text{ m}$ or less, implying a large depth extent of the Altiplano anomaly.

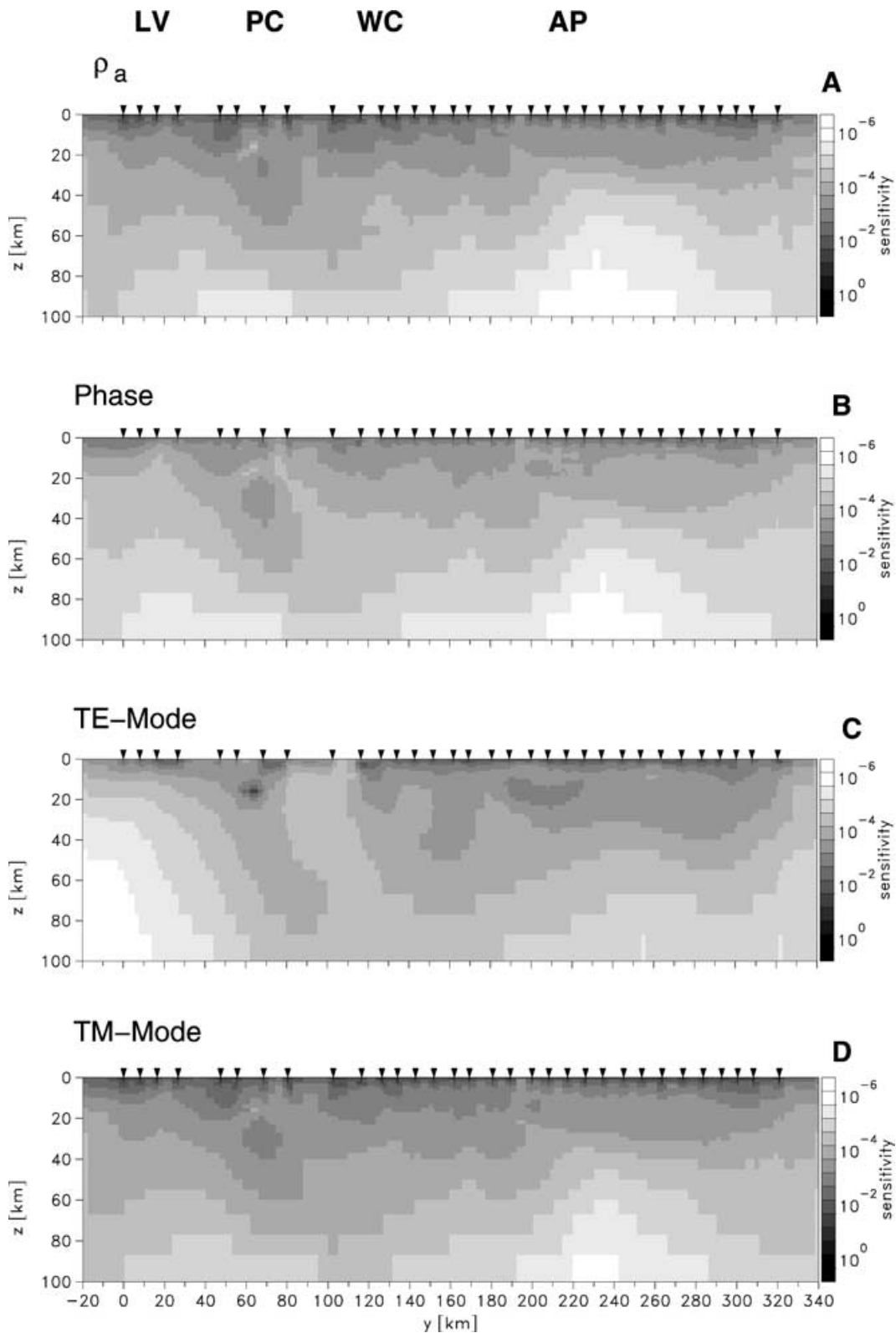


Figure 8. Partial sensitivities for ρ_a and phase (A, B), and TE and TM mode data (C, D). When normalized by standard deviation, sensitivities are comparable for ρ_a and phase. TE mode data show low sensitivity beneath the Longitudinal Valley.

Further systematic modelling was performed with the objective of better constraining the depth extent of the Altiplano anomaly. The lower boundary of the Altiplano conductor was assigned at depths of 70 and 40 km, and underlain by a 10 Ω m half-space (see Fig. 10). ρ_a

and φ curves for the ANCORP model and the two forward model responses of the characteristic site PAM are plotted below. If the section includes a 70 km deep conductor the data and model response agree to within the range of the error bars. If the conductor

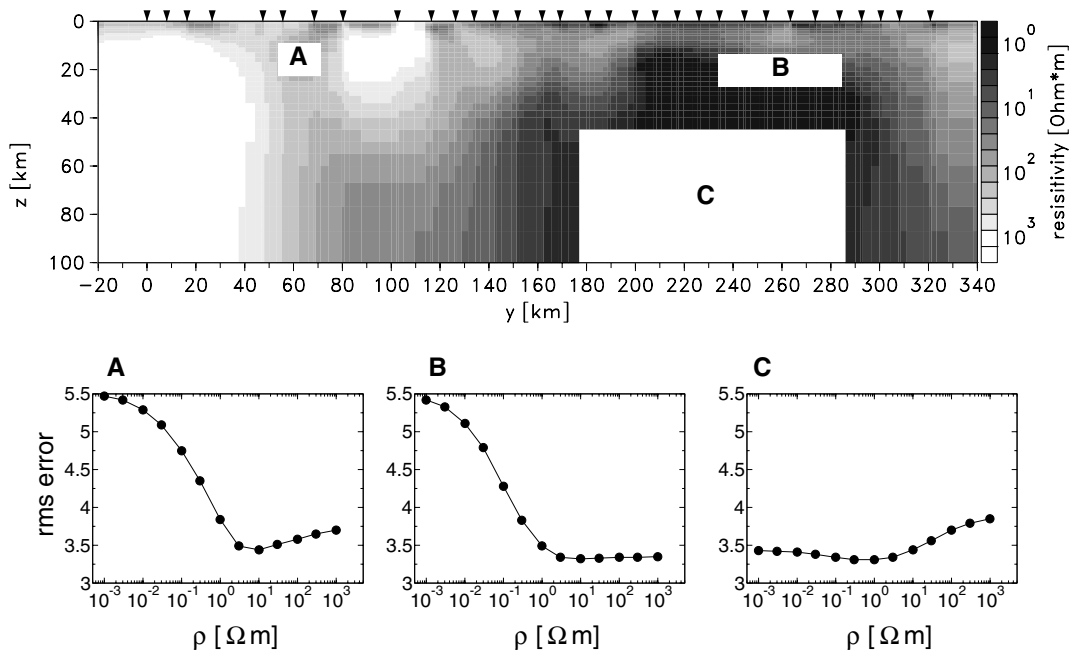


Figure 9. Sensitivity study in the style of Nolasco *et al.* (1998) for selected features of the ANCORP model. Resistivity values were varied in the marked areas over several orders of magnitude while the rest of the model remains unchanged. The rms misfit determined from forward modelling is plotted against resistivity.

is terminated at 40 km depth the computed TE mode phases are inconsistent with the data. They do not support such a shallow feature. The effect is comparable or smaller for the remaining sites on the Altiplano. However, while instructive, both the sensitivity study by Nolasco *et al.* (1998) and this modelling experiment do

not consider the dependence between model parameters, and may be inappropriate for deriving real boundaries in parameter space.

We used these two models as *a priori* information in the inversion process. As described in Section 2, the inversion algorithm preferentially seeks a model close to the *a priori* model. With the

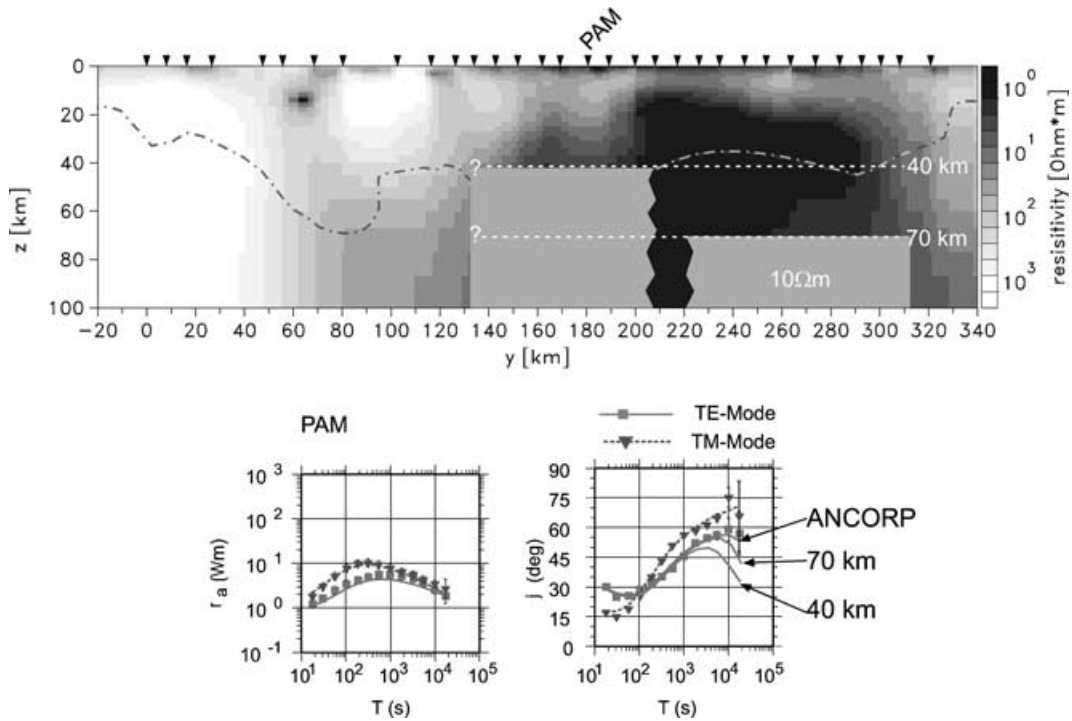


Figure 10. Systematic study to examine an assumed lower boundary of the Altiplano conductor. Data fit degrades for the TE mode phases at site PAM when fixing the boundary at 40 km while it is in the range of the error bars when fixing it at 70 km depth. Also drawn in is the 10^{-4} -isoline calculated from the linear sensitivity analysis in the preceding section.

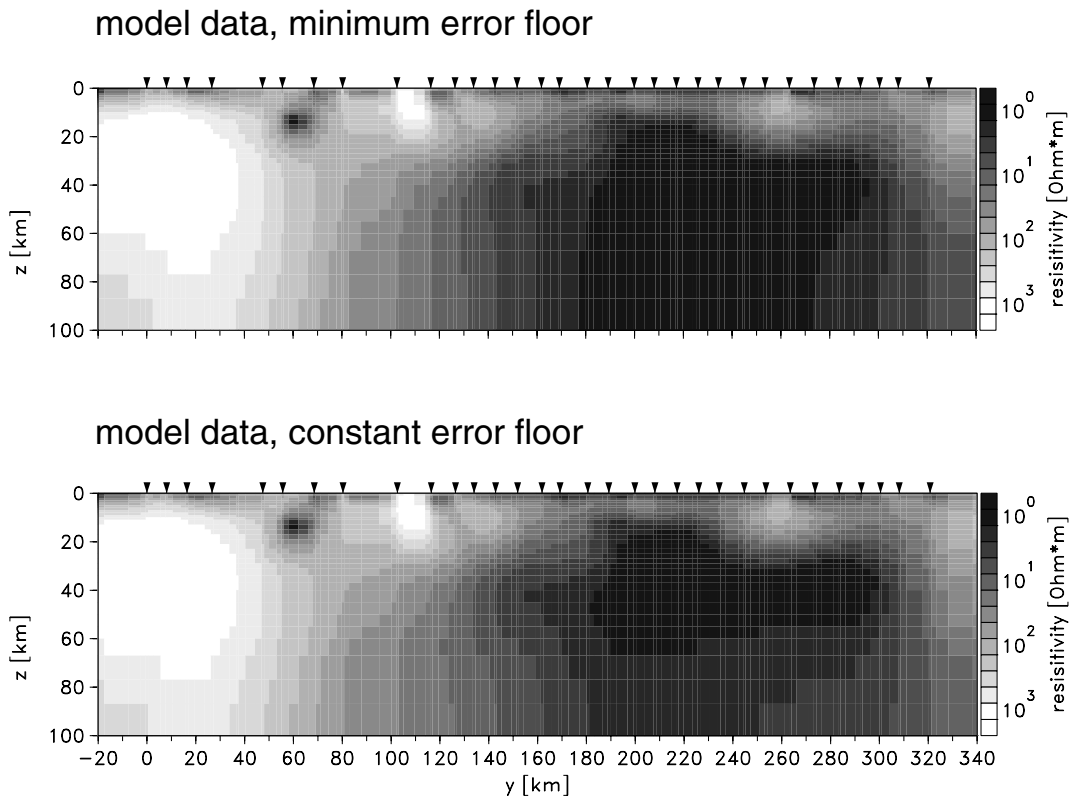


Figure 11. Synthetic data were derived from the model where the Altiplano conductor is terminated at 70 km depth (see Fig. 10) and used as input data for the inversion. Top, a minimum error floor of 20 per cent in ρ_a and 1° in φ was considered—as for the ANCORP reference model. No lower boundary can be resolved. Bottom, the same error floor was held fixed for all periods. A lower boundary can be resolved.

70 km deep conductor in the *a priori* model, the inversion result after 30 iterations (not shown here) does not significantly differ from the input information. We conclude that the data are consistent with such a model, or they are relatively insensitive to deeper parts of the Altiplano conductor. When applying the other model with the 40 km deep conductor and a $10 \Omega \text{ m}$ half-space below as an *a priori* model, this lower boundary still remains in the resulting model after 30 iterations, but resistivity values are decreased in the deeper part (also not shown here). From this we deduce that this part is more conductive than proposed by the *a priori* model. The data fit (rms) is comparable for both inversion results and the ANCORP model. Referring to the sensitivity studies in Section 3 the 10^{-4} -isoline coincides with the minimum depth extent of the Altiplano conductor derived from the systematic studies in this section, consistent with its use as a minimum limit of sensitivity.

In a further test, we calculated synthetic data from the forward model with the lower boundary of the Altiplano conductor fixed at 70 km depth. The data were assigned experimental errors, but we subject them to an error floor. A minimum error value of 20 per cent in apparent resistivities and 1° in phases was specified, as for the inversion of the ANCORP model (see Section 2). The inversion result is displayed in Fig. 11, top. In a second test we used the same synthetic data set as input, but we applied a 20 per cent, 1° error level for all periods. Consequently, the errors at the long periods are reduced (see Fig. 11 bottom for the respective inversion result). The idea is to assume a lower boundary of the Altiplano conductor and to check whether it can be resolved from the period range and data errors used. The first inversion result yields the ANCORP model, but a lower boundary can be resolved in the second case. We conclude

that the large error bars at the longest periods prevent resolution below the Altiplano at depths greater than $\sim 70 \text{ km}$.

5 COMPARISON WITH SEISMIC RESULTS

Many other geophysical experiments were performed in the Central Andes using a range of remote sensing methods. The MT profile at 21°S followed the ANCORP seismic reflection profile exactly (ANCORP Working Group 1999). In Fig. 12 we combined the MT resistivity model with a representation of seismic reflections as a line drawing (M. Stiller, GFZ Potsdam, personal communication). The Andean low-velocity zone (ALVZ) derived from receiver function analysis is also shown, which is referred to an intersection at 23°S (Yuan *et al.* 2000). An averaged sensitivity of less than 10^{-4} (which have been derived in Section 3) was used to fade out deeper model parts.

There is a good correlation between the MT and seismic results in the backarc below the Altiplano. Two reflective zones coincide with the upper boundary of the conductivity anomaly, and the gap between these zones correlates with a local plateau of the conductor. Also, the ALVZ is situated in this depth range, although it extends further westward (albeit with limited spatial resolution). A further correlation exists with high seismic attenuation derived from 2-D modelling of seismic tomography data (Schurr 2001).

No correlation exists in the forearc where the seismic image shows two strong bright-spots. There are the eastward-dipping NAZCA reflector in a depth range between 60 and 80 km, and the westward-dipping Quebrada Blanca bright-spot (QBBS) in the middle crust

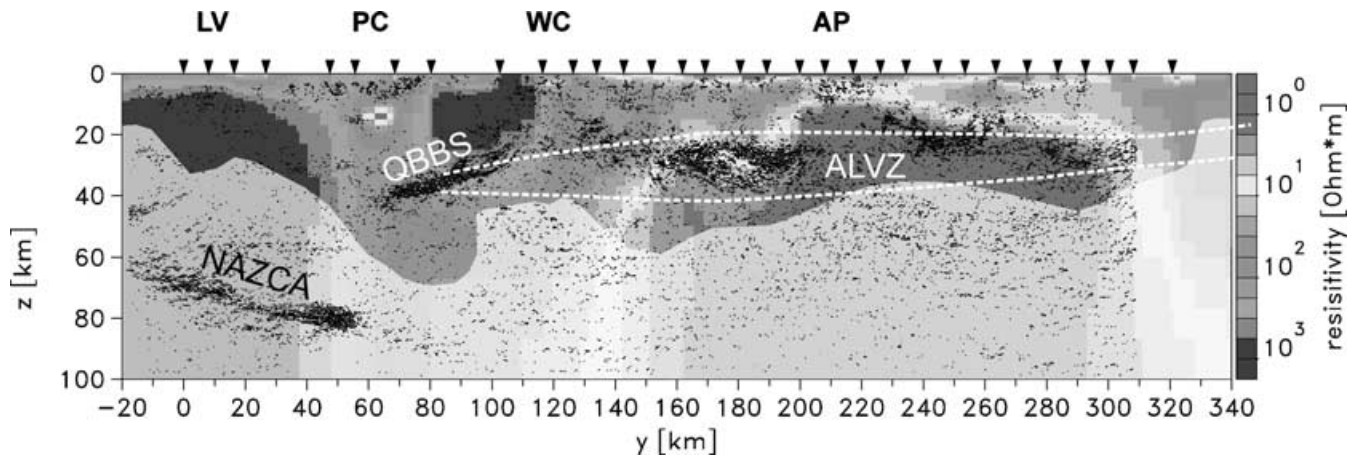


Figure 12. The ANCORP resistivity model is shown together with seismic reflections (M. Stiller, GFZ Potsdam, personal communication), and the Andean low-velocity zone (ALVZ) (Yuan *et al.* 2000) (see also Brasse *et al.* 2002). Good correlation exists in the backarc between the resolved part of the Altiplano conductor and seismic events. In contrast in the forearc, the Quebrada Blanca Bright Spot (QBBS) and the Nazca reflector associated with the down-going slab do not coincide with anomalous conductivity. Model parts with an averaged sensitivity of less than 10^{-4} have been faded out.

(ANCORP Working Group 1999). Both features are thought to be the result of fluid-related processes. The NAZCA reflector is believed to be caused by dehydration processes in the context of the down-going slab while the QBBS could originate from saline fluids ascending from this source through fracture zones probably associated with the nearby West Fissure (WF, see Fig. 2) (ANCORP Working Group 1999). If this explanation is valid, these structures should show up as high-conductivity zones in the resistivity measurements. However, neither structure coincides with any region of anomalous resistivity in the ANCORP model. As a test, we associated the seismic reflectors in the forearc with conductivity anomalies, and incorporated them as *a priori* information in the inversion process, as shown in Fig. 13 (top). We expect that *a priori* information that is either consistent with the data or cannot be resolved by the data remain almost unchanged after the inversion, while inconsistent *a priori* information should degrade. The original half-space and ocean starting model was modified by including a conductive zone in place of the QBBS (left) and in place of the down-going slab (right). These starting models were applied as *a priori* models.

The bottom models are the results after 30 iterations. Both show a similar fit to the data as the ANCORP reference model.

In the case of the QBBS (left), this *a priori* feature is still visible in the inversion model, but resistivity values were increased again towards the referring ANCORP model. The conductor beneath the Precordillera is now located at a somewhat deeper and eastward position that was postulated in the *a priori* model. Therefore, its spatial position should not be deemed to be real information. Furthermore, when inspecting the model in detail, it can be seen that high resistivities were assigned to the parts directly above and below the QBBS. This is an artefact, because within this area only an overall conductance can be resolved by the data. We therefore believe that the hypothesis of a conductive structure correlating with the QBBS is not required by the data. It should even be rejected based on the result of this test. The fact that no conductive structure coinciding with the QBBS can be found does not necessary contradict the previous interpretation of the QBBS (ANCORP Working Group 1999). Fluid-participating processes in the crust are often very complicated (e.g. Thompson & Connolly 1990). For example, other than seismic

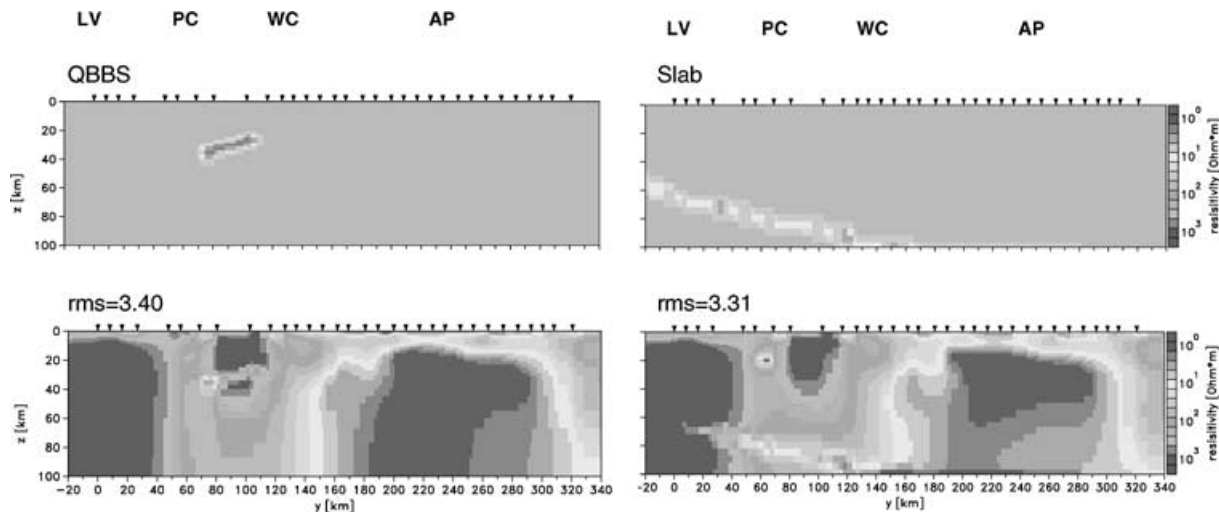


Figure 13. Top, the starting model was modified by incorporating the QBBS (left) and the down-going slab (right) as *a priori* information in the inversion process. Bottom, after performing the inversion both features remain in the model. However, the algorithm is forced to keep structural information. Resistivities are increased again for the QBBS, indicating that high conductivity is unlikely in this area. Enhanced conductivities associated with the slab cannot be ruled out by this test, but the available data are less sensitive to the respective depth.

reflectivity an observable high conductivity depends on rheological parameters such as the connectivity of the conducting phase that may not exist in this area.

In the case of the slab, this *a priori* feature vanishes in the *a posteriori* model below the Longitudinal Valley (LV), but is retained below the Precordillera, Western Cordillera and Altiplano. From this we conclude that a conductive slab cannot be completely ruled out. Other arguments indicate that it is not possible to resolve a conductive slab from on-shore data. This is clear below the Longitudinal Valley where the sensitivity is low (Figs 6 and 8C). Furthermore, model studies by Evans *et al.* (2002) show that off-shore measurements are required, which would be more sensitive to the existence of a conducting slab.

Another interesting aspect is that a lower boundary of the Altiplano conductor can be resolved, if another deeper conductive structure is assumed. This conclusion can be taken into account as an alternative result, but it cannot be resolved by the MT data.

6 DISCUSSION AND CONCLUSIONS

A 2-D resistivity model for the Central Andes has been derived by inversion of magnetotelluric data. It is an inversion result in terms of a minimum structure model. This means that the model represents a compromise between model smoothness and optimal data fit, an approach that in our opinion best suits the character of magnetotelluric data, which show integrative behaviour rather than high structural resolution power. Data analysis, the treatment of field data and the causes of anomalous conductivities (or its absence) have been discussed in Brasse *et al.* (2002).

The model that we call the ANCORP model shows a remarkable conductivity anomaly in the backarc of the South American subduction zone below the Bolivian Altiplano. This anomaly is outstanding in both dimension and conductivity. Owing to a smoothness constraint considered in the objective function the anomaly extends to a mantle depth greater than 100 km. Another comparatively small-scaled and localized anomaly exists in the crust beneath the Precordillera. In contrast to magnetotelluric surveys in other subduction zones (e.g. Kurtz *et al.* 1986; Wannamaker *et al.* 1989), the ANCORP model shows no correlation between the down-going plate and a zone of enhanced conductivity. Indeed, the resistivity values are high in this region. The corresponding volcanic front shows up with high resistivity values that differ from 2-D modelling results at 22°S (Schwarz & Krüger 1997), who found high conductivities below the Western Cordillera.

It is known that in magnetotellurics the inverse solution need not be unique, and a large number of possible models exist, explaining the observations within a given error range. From inversion alone it is therefore not clear which model features are really required by the data, an important question for the model interpretation, and for the comparison with other geophysical results. This paper has shown that sensitivity studies are a necessary and helpful tool in increasing the reliability of models. They were performed in order to determine how malleable the model is in terms of derived resistivity values and model structure. Generally, these studies are based on forward modelling in a trial and error style. We applied these non-linear techniques to the ANCORP model as well as a new approach that we characterize as linear sensitivity studies. These linear studies depend on the calculation of average sensitivities from the sensitivity matrix. While the systematic, i.e. non-linear studies, do not take complicated parameter dependences into account, the linear studies are only of value close to the respective model. In combination, and together

with the consideration of different *a priori* models and synthetic data sets in the inversion process, they reveal a more reliable picture of the entire ANCORP model.

In particular, we found that the Altiplano conductor can be resolved to depths of at least 50 km using the available data. This was not clear from inversion alone where this structure seems to be extended to depths greater than 100 km. To obtain more information higher data quality at long periods is necessary, which requires measuring times of several months. Also, it cannot be definitely excluded that a structure of significantly less vertical extent could also explain the Altiplano conductivity anomaly. In that case an even higher conductivity must be assumed, which requires extreme petrophysical conditions (Schilling *et al.* 1997). Below the Longitudinal Valley sensitivity is small. At first this is not consistent with the high resistivity values in this area, and hence the expected greater penetration depth. A plausible explanation for this is its location between two extremely good conductors, namely the Altiplano anomaly and the Pacific Ocean. This makes it difficult to discriminate the effects of these anomalies from smaller conductors at depth, thus reducing the associated sensitivities. In particular, the currents running parallel to the trench (TE mode) flow preferably in the ocean layer, which results in low sensitivity, and may explain the absence of a good conducting slab. The localized conductor beneath the Precordillera is a very sensitive model feature and can even be seen in a single-site sensitivity presentation far away from this feature. However, the existence of this conductor is well documented, but because of the three-dimensionality of the data its vertical position cannot be sufficiently resolved by 2-D modelling. Lezaeta (2001) and Soyer & Brasse (2001) derive a shallower location for this conductor from 3-D forward modelling and intersite geomagnetic transfer function analysis.

We also compared the ANCORP model with results from seismic measurements, showing a good correlation in the backarc between patterns of seismic reflectivity (M. Stiller, GFZ Potsdam, personal communication), the Andean low-velocity zone (Yuan *et al.* 2000), high seismic attenuation (Schurr 2001), and the resolved part of the Altiplano conductor. The two main seismic features in the forearc (Quebrada Blanca Brightspot, NAZCA reflector) (ANCORP Working Group 1999) do not coincide with anomalous resistivity zones. Both were interpreted as indicating fluid-related processes. It was questionable whether this anticorrelation is caused by the lack of sensitivity provided by the magnetotelluric data, or different petrophysical properties. We incorporated these features as *a priori* information in the inversion process, and concluded from the resulting models that the assumption of a conductive structure correlating with the QBBS is not consistent with the MT data, while the existence of a conducting slab cannot be completely ruled out.

ACKNOWLEDGMENTS

The data set was collected within the framework of the Collaborative Research Project SFB 267 *Deformation Processes in the Central Andes*. We would like to thank R.L. Mackie who provided the 2-D inversion code, R. Holme for major revisions, and H. Brasse for many useful ideas. We also thank R.N. Edwards who was very helpful with the revision of the manuscript.

REFERENCES

- ANCORP Working Group, 1999. Seismic reflection image revealing offset of Andean subduction-zone earthquake locations into oceanic mantle, *Nature*, **397**, 341–344.

- Björk, Å., 1996. *Numerical Methods for Least Squares*, SIAM, Philadelphia.
- Brasse, H., Lezaeta, P., Rath, V., Schwalenberg, K., Soyer, W. & Haak, V., 2002. The Bolivian Altiplano conductivity anomaly, *J. geophys. Res.*, in press.
- de Groot-Hedlin, C. & Constable, S., 1990. Occam's inversion to generate smooth, two-dimensional models for magnetotelluric data, *Geophysics*, **55**, 1613–1624.
- Evans, R.L., Chave, A.D. & Booker, J.R., 2002. On the importance of offshore data for magnetotelluric studies of ocean–continent subduction systems, *Geophys. Res. Lett.*, in press.
- Farquharson, C.G. & Oldenburg, D.W., 1996. Approximate sensitivities for the electromagnetic inverse problem, *Geophys. J. Int.*, **126**, 235–252.
- Hadamard, J., 1923. *Lectures on the Cauchy Problem in Linear Partial Differential Equations*, Yale University Press, New Haven.
- Hansen, P.C., 1998. *Rank Deficient and Discrete Ill-Posed Problems. Numerical Aspects of Linear Inversion*, SIAM, Philadelphia.
- Kurtz, R.D., Delaurier, J.M. & Gupta, J.C., 1986. A magnetotelluric sounding across Vancouver Island detects the subducting Juan de Fuca plate, *Nature*, **321**, 596–599.
- Lezaeta, P., 2001. Distortion analysis and 3-D modeling of magnetotelluric data in the Southern Central Andes, *PhD thesis*, Free University of Berlin.
- Mackie, R.L. & Madden, T.R., 1993. Three-dimensional magnetotelluric inversion using conjugate gradients, *Geophys. J. Int.*, **115**, 215–229.
- Mackie, R., Rieven, S. & Rodi, W., 1997. *Users Manual and Software Documentation for Two-Dimensional Inversion of Magnetotelluric Data*, GSY-USA, Inc., San Francisco, CA 94114, User Documentation.
- Madden, T.R., 1972. Transmission systems and network analogies to geophysical forward and inverse problems, 72–3, Dept of Geology and Geophysics, MIT, Cambridge, MA.
- McGillivray, P.R. & Oldenburg, D.W., 1990. Methods for calculating Frechet derivatives and sensitivities for the non-linear inverse problem; a comparative study, *Geophys. Prospect.*, **38**, 499–524.
- Nolasco, R., Tarits, P., Filloux, J. & Chave, A., 1998. Magnetotelluric imaging of the Society Islands hotspot, *J. geophys. Res.*, **103**, 287–309.
- Oldenburg, D. & Li, Y., 1999. Estimating depth of investigation in DC resistivity and IP surveys, *Geophysics*, **11**, 403–416.
- Rodi, W. & Mackie, R.L., 2001. Nonlinear conjugate gradients algorithm for 2-D magnetotelluric inversions, *Geophysics*, **66**, 174–187.
- Schilling, F.R., Partzsch, G.M., Brasse, H. & Schwarz, G., 1997. Partial melting below the magmatic arc in the Central Andes deduced from geoelectromagnetic field experiments and laboratory data, *Phys. Earth planet. Inter.*, **103**, 17–32.
- Schurr, B., 2001. Seismic structure of the Central Andean subduction zone from local earthquake data, *PhD thesis*, GFZ Potsdam Scientific Technical STR 01/01.
- Schwarz, G. & Krüger, D., 1997. Resistivity cross-section through the southern Central Andes as inferred from magnetotelluric and geomagnetic deep soundings, *J. geophys. Res.*, **102**, 11 957–11 978.
- Soyer, W. & Brasse, H., 2001. A magneto-variation array study in the Central Andes of N Chile and SW Bolivia, *Geophys. Res. Lett.*, **28**, 3023–3026.
- Tarantola, A. & Valette, B., 1982a. Inverse problems = quest for information, *J. Geophys.*, **50**, 159–170.
- Tarantola, A. & Valette, B., 1982b. Generalized nonlinear inverse problems solved using the least-squares criterion, *Rev. Geophys. Space Phys.*, **20**, 219–232.
- Thompson, A.B. & Connolly, J.A.D., 1990. Metamorphic fluids and anomalous porosities in the lower crust, *Tectonophysics*, **182**, 47–55.
- Tikhonov, A.N. & Arsenin, V.Y., 1979. *Methods for Solving Ill-Posed Problems*, Nauka, Moscow.
- Wannamaker, P.E., Booker, J.R., Jones, A.G., Chave, A.D., Filloux, J.H., Waff, H.S. & Law, L.K., 1989. Resistivity cross-section through the Juan de Fuca subduction system and its tectonic implications, *J. geophys. Res.*, **94**, 14 127–14 144.
- Yuan, X. *et al.*, 2000. Subduction and collision processes in the Central Andes constrained by converted seismic phases, *Nature*, **408**, 958–961.